Contactless Blood Pressure Measurement via Remote Photoplethysmography with Synthetic Data Generation Using Generative Adversarial Network

Bing-Fei Wu[1], Li-Wen Chiu[1], Yi-Chiao Wu[1], Chun-Chih Lai[1], and Pao-Hsien Chu[2]

[1]Institute of Electrical and Control Engineering, National Yang Ming Chiao Tung University
[2]Chang Gung Memorial Hospital, Chang Gung University

{bwu,joiewu}@cssp.cn.nctu.edu.tw, {lili0519.ee07,cclai.ee10}@nycu.edu.tw

Abstract

Deriving blood pressure in a non-invasive way via photoplethysmography (PPG) signals has become a familiar topic. With the knowledge of the relation between PPG and blood pressure, we expect to further make the measurement contactless for convenience reasons. An alternative signal source is remote photoplethysmography (rPPG) signals. There are mainly two kinds of approaches for exploiting blood pressure through PPG signals, one is by calculating the pulse transit time of the arterial pulse wave at two consecutive sites and the other is based on waveform feature analysis from a single signal. The calibration procedure is necessary for the former way, which leads to some limitations in general use. On the other hand, the properties of the rPPG waveform are far from PPG signals. Hence, the known waveform features in PPG signals are hard to be leveraged in the case of rPPG signals. Recently, convolutional neural networks are also applied for solving this problem. However, the lack of data is an obstacle to the training procedure and evaluation. In this study, a multi-channel rPPG-based blood pressure estimator is proposed. To ease the data scarcity issue, the generative adversarial network is adopted to augment synthetic waveform data. Besides, as we know that some physiological states like age and BMI are dominant factors in blood pressure. InfoGAN is chosen in this work to generate the synthetic data with the blood pressure value fluctuating correspondingly to the controlled age and BMI combination. The proposed model outperforms the state-of-the-art methods on MIMIC III and Cuffless datasets. With the synthetic data generation, the mean absolute error (MAE) is reduced to 6.72 *and* 5.95 *mmHg in MAP and DBP respectively. The standard deviations of the MAEs are also reduced. In the rPPG case, the MAE of SBP is* 9.13 *and* 8.76 *mmHg for DBP.*

1. Introduction

Blood pressure is an important vital indicator. The common non-invasive measurement is through a blood pressure cuff [1, 15, 26]. To further overcome the contact measuring limitation, in some studies, the time or phase difference, e.g., pulse transit time (PTT) extraction, is leveraged to estimate blood pressure value. The original definition of PTT is the traveling time difference of the arterial pulse wave between two consecutive sites. To capture the more significant time interval, central aortic and peripheral vessels are chosen as observed sites. Hence, electrocardiographic (ECG) and photoplethysmography (PPG) signals of the fingertip or the ear lobe are recorded respectively. The R or Q wave of the ECG signal has been used as the starting point. Conventionally the point on the PPG pulse waveform which is approximately 50% of the height of the maximum value indicates the arrival time [10, 22, 25]. In addition, the alternative signal sources can be multiple PPGs rather than ECG and PPG signals [13, 14, 16, 18].

Furthermore, for contactless measuring, the rPPG signals are taken into account [23]. It is worth noticing that, PTT-based approaches can only obtain the blood pressure change but not a certain value. That is, the calibration procedure that is correlated to the distance between the two observation sites is necessary for this kind of method [3]. To ease the measurement, the single signal source methods are introduced.

For a single signal source, the blood pressure can be derived from waveform features, like derivatives or morphology of the blood volume waveform. Slapničar et al. [21] use a deep neural network with the first and second derivatives of the PPG signals as input signals to predict blood pressure. Chakraborty et al. [4] analyze the PPG waveform to extract the feature contained pulse wave velocity (PWV) information and regress the blood pressure value. Haddad et al. [7] predict blood pressure via a multi-linear regression

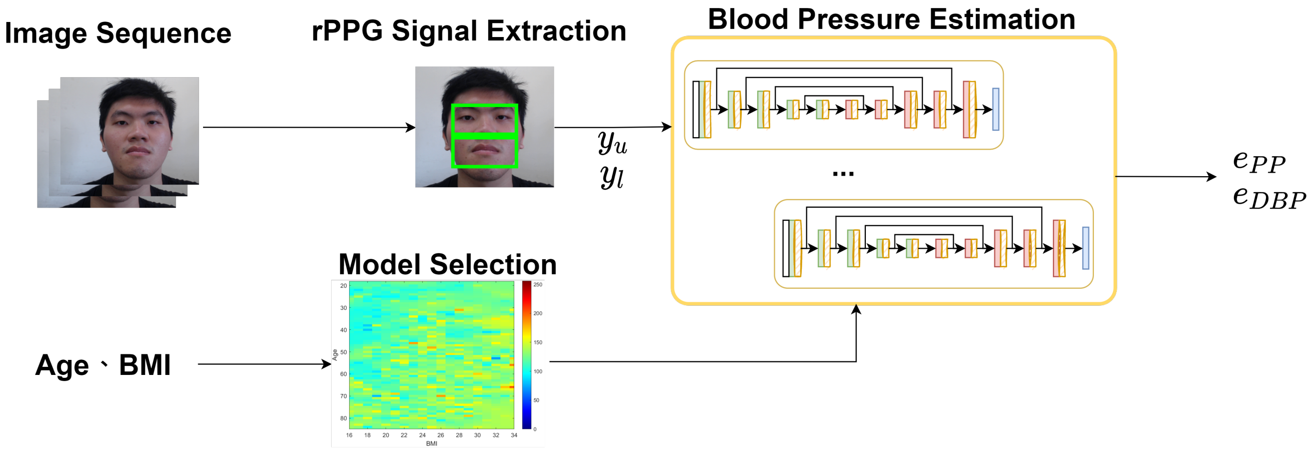

Figure 1. The overall structure of blood pressure estimation.

approach with inputs consisted the first and second derivative of single PPG signals. Zhou et al. [27] extract valid peaks and valleys of rPPG and adopt their averages and BMI as features fitting BP by the linear regression model. Rong et al. [19] adopt more features from rPPG, including area, slope, energy, etc. as a neural network input to predict blood pressure value.

However, the morphological properties of the rPPG signals may be far from the ones of the PPG signals because arterial pulse waveform changes along the arterial tree. As the vascular elasticity difference between central aortic and peripheral vessels, some subtle features barely exist in rPPG signals.

Besides the hand-crafted waveform features, convolutional (CNN) or recurrent neural network (RNN) is applied for high-leveled PPG feature extraction. As the model maps the PPG signals into blood pressure values in one-stage, these are called end-to-end approaches. Han et al. [8] train a multi-tasks CNN model to extract PPG features. The features are concatenated with BMI information to predict the hypertension classification and blood pressure at the same time. Schrumpf et al. [20] obtain PPG or rPPG signal with better quality by filtering and calculating SNR, predicting BP based on classical networks including AlexNet, ResNet, and LSTM. In [24], the multi-channel rPPG signals, heart rate value, and BMI are fed into a CNN model that is modified from ResNet18 [9]. Afterward, a training procedure loop is applied to fine-tune the model fitting the signals which are filtered in varying band-pass filters.

Since CNN-based or RNN-based models are data-driven, there are the following limitations due to the characteristics. The clean and abundant training data is hard to collect especially for rPPG. On the other hand, the model outputs are easily bounded by the distribution of the training data. For example, the model is prone to estimate the value that appears commonly. As the result, larger errors occur in the group of hypertension, which is not feasible in practical usage.

To take both advantages from PTT-based and waveform-based approaches, in this study, a multi-channel end-to-end model is proposed. The rPPG signals from the upper and lower half face are leveraged as the model input which contains the information of phase difference and more waveform features. The encoder-decoder architecture with symmetric skip connection is applied as the backbone model that is able to filter out the noise carried on signals efficiently and maintain a slight model size simultaneously.

For easing the mentioned data-driven issues in model training, the synthetic data generation with the generative adversarial network (GAN) is integrated into the training strategy. Additionally, with our knowledge of the relation between age, BMI, and blood pressure, the augmented data is expected to fluctuate correspondingly to the subject information. That is, as the age or BMI is higher, the blood pressure is probably higher. Hence, the idea of InfoGAN [5] is adopted here for generating training data with controlled specifically age and BMI combination that is missing in the collection. With the synthetic data, the model outputs can be distributed in a wider range and handle the cases in the hypertension group.

This paper is organized as follows. In Section 2, the proposed method, including the backbone architecture, the training strategy with InfoGAN [5] and the multi-model structure are addressed. The assessment details, the dataset description and the experimental results are shown in Section 3. Finally, the conclusion is given in Section 4.

2. Proposed Method

2.1. Overall Structure

The overall structure of the proposed method is shown in Figure 1. With the sequence input facial images, the face detection and the region of interest (ROI) alignment are applied to get the upper and lower face first. After chrominance-based (CHROM) [6] rPPG extraction, we obtain two rPPG signals of the upper and lower face, y_u and y_l, respectively. To filter out the noise and extract high-level waveform feature simultaneously, an encoder-decoder architecture backbone model with multi-channel rPPG input is addressed in Section 2.2.

Besides, with the observation of the existing end-to-end blood pressure estimators, an issue to be reckoned with is the bounded distribution correspondingly to the lack of training data. As the range of the systolic blood pressure (SBP) of human beings covers about $[90, 200]$ that is relatively wide. Conventionally, the output of the CNN-based model is prone to lie in the narrow band around the average of the blood pressure range. As the results, the estimation error increases for the group with boundary blood pressure values, like hypertension.

For ease of training difficulties, the known relation between the physiological status and the blood pressure is leveraged. The status of age and BMI, which is accessible commonly and easily for practical usage, is chosen as the assistance of a multi-model blood pressure estimation structure. The entire range of the blood pressure is first sliced into 10 pieces equally and makes 10 models to be heeded on certain smaller ranges. Based on the age and the BMI, a rough range is recorded with the mapping table, that is, the appropriate model is picked. The details of mapping table construction are introduced in Section 2.3.

Finally, a synthetic data generation with InfoGAN [5] is employed to further solve the mentioned issue of data scarcity. During the augmentation procedure, age and BMI are regarded as two controlled factors so that the synthetic blood pressure fluctuates correspondingly. As the data distribution can be handled, the model training procedure is enhanced still further. In Section 2.4, the training tricks for synthetic data generation is addressed.

2.2. Backbone Architecture

An encoder-decoder architecture is designed as the backbone model. The symmetric skip connection ensures the waveform feature not to vanish as the depth of the model increases, which is capable to filter out the noise and interference carried on the rPPG signals. The diagram of the backbone model is shown in Figure 2. There are both 5-layered, 1D convolution for encoder and 1D transpose convolution (or de-convolution) for decoder respectively, and the activation function is PReLu. In Table 1, the implementation, the corresponding output size and the number of the parameters of each model are listed.

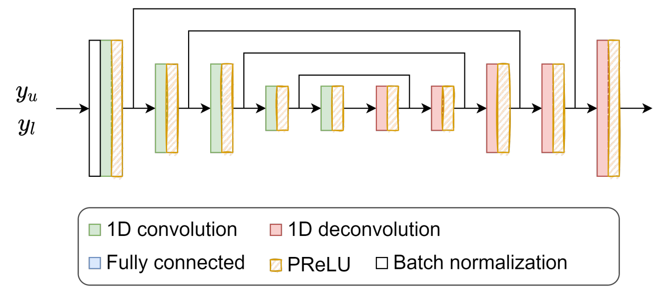

Figure 2. The model architecture of the backbone model, F.

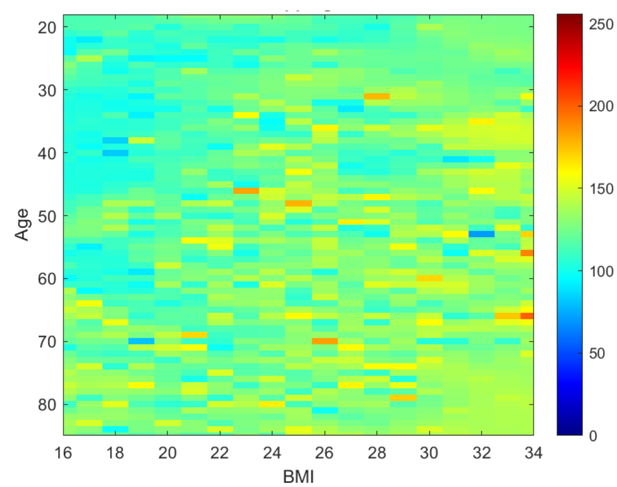

Figure 3. The SBP mapping table for model selection, F.

2.3. Model Selection

According to our knowledge, BMI and age are two main factors affecting blood pressure. Thus, we statistic age, BMI, and systolic blood pressure for all of the subjects in training dataset to create an SBP mapping table $M(Age, BMI)$. The age range is from 18 to 85 and the BMI range is from 16 to 34. The value interval in the range is 1. The interpolation is applied to fill the mapping table for specified age and BMI combinations that are missing in the collection. Finally, the obtained mapping table which is used for BP model selection is shown in Figure 3. The horizontal axis is BMI, the vertical axis is Age, and different SBP values are represented by color.

The SBP range considered in this study is from 90 to 160, we partition it into 10 intervals evenly. Each interval corresponds to different BP models. We can obtain the selected model ID $Model_{ID}$ through the following formula:

$$Model_{ID} = \lfloor (M(Age, BMI) - 90)/7 \rfloor \quad (1)$$

where $M(\cdot) \in [90, 160]$ is denoted as the mapping table.

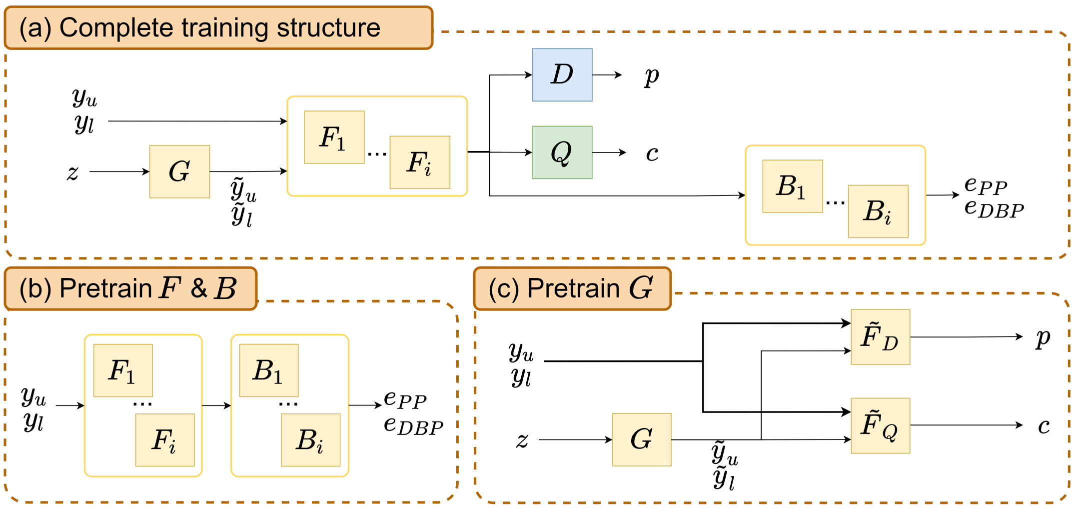

Figure 4. The training structure of synthetic data generation.

Table 1. The implementation detail of the models.

Model	Layer	Output Size	Parameters
F	BN	[1, 2, 512]	86.93K
	Conv1D_1	[1, 8, 449]	
	Conv1D_2	[1, 16, 396]	
	Conv1D_3	[1, 24, 349]	
	Conv1D_4	[1, 32, 338]	
	Conv1D_5	[1, 40, 333]	
	ConvTranspose1D_1	[1, 32, 338]	
	ConvTranspose1D_1	[1, 24, 349]	
	ConvTranspose1D_1	[1, 16, 396]	
	ConvTranspose1D_1	[1, 8, 449]	
	ConvTranspose1D_1	[1, 2, 512]	
G	Conv1D_1	[1, 1024, 1]	3.95M
	Conv1D_2	[1, 128, 25]	
	Conv1D_3	[1, 128, 116]	
	Conv1D_4	[1, 64, 248]	
	Conv1D_5	[1, 2, 512]	
Q	Linear_1	[1, 256]	262.66K
	Linear_mean	[1, 1]	
	Linear_var	[1, 1]	
D	Linear	[1, 1]	1.03K
B	Linear	[1, 2]	2.05K

The activation function leveraged here is PReLu.

2.4. Synthetic Data Generation

For generating more data to assist the model training, we adapt the InfoGAN [5] which is able to generate certain data by learning the mutual information between latent noise and the observation. As shown in Figure 4, F is the feature extractor and B is the regression model. The inputs are 2-channel rPPG signals of the upper and the lower face y_u, y_l. The outputs are the estimated pulse pressure (PP) e_{PP} and diastolic blood pressure (DBP) e_{DBP}. The estimated SBP e_{SBP} is calculated via the equation:

$$e_{SBP} = e_{DBP} + e_{PP} \tag{2}$$

The generator is G with the input noise z composed of the incompressible and semantic part. And $\tilde{y_u}$, $\tilde{y_l}$ is denoted as the output which is fake rPPG data. The discriminator is composed of F and D and p is the output prediction of whether the input signal is fake or real. The F and Q is the auxiliary discriminator to extract the mutual information between latent code and generated signal. The output c of F and Q, which is discrete noise here, is expected to learn the characteristic of age and BMI. That helps to generate the lacking data in the collected dataset and elevate the model's ability with rare data.

With definition $\tilde{D} = D \cdot F$, $\tilde{Q} = Q \cdot F$ and $\tilde{B} = B \cdot F$, the objective function for original GAN is define as:

$$\min_G \max_{\tilde{D}} \mathcal{L}_{\text{GAN}}(\tilde{D}, G) \tag{3}$$

And in the case of InfoGAN, the objective function is:

$$\min_{G,\tilde{Q}} \max_{\tilde{D}} \mathcal{L}_{\text{GAN}}(\tilde{D}, G) - \lambda_1 \mathcal{L}_{\text{Info}}(G, \tilde{Q}) \tag{4}$$

Hence, the final objective function of the overall training is

$$\min_{G,\tilde{Q},\tilde{B}} \max_{\tilde{D}} \mathcal{L}_{\text{GAN}}(\tilde{D}, G) - \lambda_1 \mathcal{L}_{\text{Info}}(G, \tilde{Q}) - \lambda_2 \mathcal{L}_{BP} \tag{5}$$

with two hyper parameters λ_1 and λ_2.

The $\mathcal{L}_{\text{GAN}}(\tilde{D}, G)$ is given by the following equation

$$\mathcal{L}_{\text{GAN}}(\tilde{D}, G) = \mathbb{E}_{y \sim P_{\text{real}}}[\log(\tilde{D}(y))] + \mathbb{E}_{z \sim P_z}[\log(1 - \tilde{D}(G(z)))] \tag{6}$$

where P_{real} is the real data distribution and P_z the noise distribution.

The $\mathcal{L}_{\text{Info}}(G, \tilde{Q})$ is given by

$$\mathcal{L}_{\text{Info}}(G, \tilde{Q}) = \mathbb{E}_{c \sim P(c), y \sim G(z,c)}[\log \tilde{Q}(c \mid y)] + H(c) \quad (7)$$

where c denotes latent code, $\tilde{Q}(c \mid y)$ denotes the approximation of $P(c \mid y)$, and $H(c)$ is the entropy of the latent code which can treated as a constant by fixing the latent code distribution.

The $\mathcal{L}_{BP}$ is defined as

$$\mathcal{L}_{BP} = \left\| e_{PP} - \hat{t}_{PP} \right\|_2^2 + \left\| e_{DBP} - \hat{t}_{DBP} \right\|_2^2 \quad (8)$$

where $\hat{t}_{PP}$ is the target value of pulse pressure and $\hat{t}_{DBP}$ denotes the target value of diastolic pressure.

In the implementation, the model F, B and G are pretrained with the training structure shown in the subfigure (b) and (c) in Figure 4. This pretrained step is aim to obtain a generator with prerequisite capacities to generate fake rPPG signals and a series of F and B with the prior ability of blood pressure estimation. The models finetuned with the pretrained weights tend to converge to better result.

3. Experimental Results

3.1. Training Details

The proposed method is implemented with the deep learning framework PyTorch [17]. The optimizer is Adam and the learning rate is 2×10^{-3} for all of the models. Both of the hyper-parameters λ_1 and λ_2 are set to 1 in the following experiments.

3.2. Dataset Description

3.2.1 MIMIC III Dataset

MIMIC III Dataset [11] comprises thousands of signal records collected by various hospitals between 2001 and 2008. Each signal were sampled at 125Hz with at least 8-bit accuracy. We extracted PPG and arterial blood pressure (ABP) signals from the database and remove the signals having many flat parts or invalid values due to different distortions and artifacts in signals.

3.2.2 Cuffless Dataset

Cuffless Dataset is a small fraction of the MIMIC II, containing $12,000$ preprocessed and cleaned records, provided by Kachuee et al. [12]. Each record is consist of ECG, PPG, and ABP signals sampled at 125Hz.

We apply both datasets for attesting the baseline performance of the proposed encoder-decoder architecture on BP prediction based on PPG waveform and the capability of the proposed training strategy to alleviate the data-driven issue.

3.2.3 rPPG Dataset

To conduct the assessment on the rPPG case, we cooperate on an institutional review board with Chang Gung Medical Foundation, Taiwan to collect the data for camera-based blood pressure estimation. Figure 5 shows age, BMI, SBP, and DBP distribution in the rPPG dataset. There are $1,138$ participants in the dataset which contains 860 males and 278 females ages from 18 to 92. Each subject is recorded for 80 seconds and the camera is set in the distance of about 60 cm. The camera is Logitech C920 and the facial images are recorded in the size of 640×480 with 30FPS 8-bit lossless format. The ground truth of the blood pressure is measured by a mercury sphygmomanometer. It is worth noticing that, the participants within this rPPG dataset are composed of patients with hypertension, diabetes, cardiac disease, etc.

3.3. Assessment Details

Since the MIMIC III dataset and Cuffless dataset do not provide age and BMI information, the proposed multi-model structure cannot be applied. Furthermore, there is no one to evaluate the performance of the blood pressure prediction for these two datasets using multi-model structure in related work. Thus, we adopt a single-model structure without model selection based on BMI and age information to verify the performance of our backbone model and training strategy in predicting blood pressure with only PPG signals.

The training procedure is shown in Figure 6. As same as the training process of multi-model structure, we first train the single-model structure consisting of feature extractor F and regression module B. Instead of 2 rPPG signals obtained from the upper and lower part of faces, the single PPG signal y is as model input. The pre-train model in the first stage will be our baseline performance of BP prediction. Second, we utilize InfoGAN train a generator G for synthetic PPG signal generation. The pre-trained models are finetuned in the third stage.

Protocol of each dataset are shown in Table 2. For the fair competition, we have randomly drawn $250,000$ samples for testing from 625 subjects, $1,000,000$ samples for training from the rest subjects in the MIMIC dataset [20]. Each subject contributed the same number of samples. In the Cuffless dataset [12], we randomly sample $4,254$ records as our dataset under ensuring the same distribution, and we use the identical proportion $6:2:2$ to split the dataset into training, validation, and testing. For the rPPG dataset, we randomly smaple same number of subjects from normal, prehypertension, hypertension states as testing data, total are 177, the rest are used for training.

3.4. Results

The experiments on PPG and rPPG datasets are both conducted, the former ones are leveraged to verify the ef-

Table 2. The overall dataset description.

Dataset	Signal Type	Protocol		Multi-Model w/ Age & BMI	Reference
		Trainging Data	Testing Data		
MIMIC III [11]	PPG	1,000,000 samples	250,000 samples	X	Schrumpf et al. [20]
Cuffless [12]	PPG	2,552 samples	851 samples	X	Kachuee et al. [12]
rPPG Dataset	rPPG	961 subjects	177 subjects	V	self-constructed

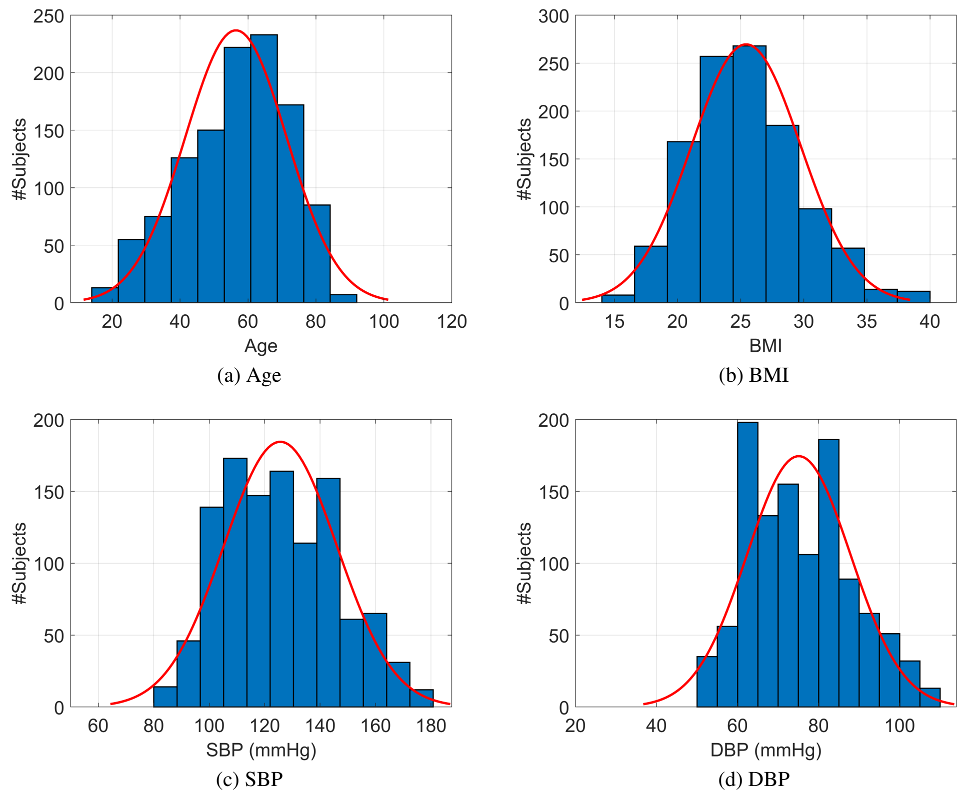

Figure 5. Distribution of rPPG Dataset

Table 3. Comparison results of MAE (mmHg) on MIMIC III dataset.

Approach		SBP	DBP
Schrumpf et al. [20]	Mean-Regressor	19.60	9.80
	AlexNet	16.60	8.70
	ResNet	16.40	8.50
	LSTM	16.40	8.60
Slapničar et al. [21]		16.80	8.80
Ours (Baseline)		14.82	7.31
Ours (w/ InfoGAN)		**14.26**	**7.11**

ficiency of the backbone model, and the latter shows the overall performance of the proposed method.

There are two public PPG datasets are considered in the assessment, including MIMIC III [11] and Cuffless [12] dataset. The results on MIMIC III dataset are shown in Table 3, it shows that our backbone model outperforms other PPG-based approaches as the MAE reduces about 2 mmHg. Furthermore, the MAE of SBP achieves lower at 14.26 mmHg with the assistance of the synthetic data with InfoGAN.

The experimental results on Cuffless dataset [12] demonstrate the same trend with the ones on MIMIC III. As presented in Table 4, the proposed method reaches the smallest MAE at 5.95 mmHg for DBP, 10.59 mmHg for SBP and 6.72 mmHg for the mean arterial pressure (MAP) re-

Table 4. Comparison results on Cuffless dataset.

Approach		DBP(mmHg)		MAP(mmHg)		SBP(mmHg)	
		MAE	Std	MAE	Std	MAE	Std
Kachuee et al. [12]	RLR_{LF}	7.24	9.23	9.34	11.79	14.73	18.47
	RLR_{PF}	7.42	10.02	8.50	10.91	14.46	18.17
	ANN	6.86	8.96	8.84	11.24	13.78	17.46
	SVM	6.34	8.45	7.52	9.54	12.38	16.17
Ours (Baseline)		6.23	5.93	7.06	6.02	11.32	9.10
Ours (w/ InfoGAN)		**5.95**	**5.76**	**6.72**	**5.88**	**10.59**	**9.07**

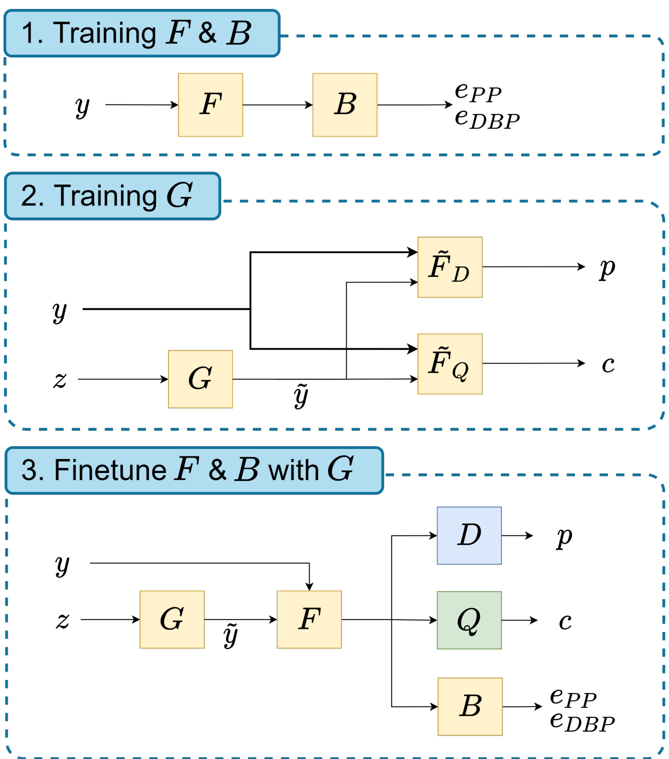

Figure 6. The training procedure of synthetic data generation for PPG signals.

spectively. Besides, the standard deviation of MAE is decreased to about one-half with the proposed backbone model. That is this model architecture efficiently eases the issue of bounded output in a certain range around average.

On the other hand, the results of the assessment conducted on the rPPG dataset are shown in Table 5. It is worth noticing that, as the rPPG dataset is self-constructed, the physiological states like age and BMI of the participants are recorded as well. The proposed model without prior knowledge of age and BMI can also achieve the lowest MAE among all existing approaches. Besides, our backbone model architecture is relatively slighter. Take FS2-Net [24] for example, due to its second-best performance, the number of the parameter in FS2-Net is $1130.24K$, which is much larger than the single backbone model which is with the size of $87.96K$. Furthermore, with model selection procedure, the MAE can be further reduced to 10.15 and 8.84 mmHg for SBP and DBP.

Table 5. Comparison results on rPPG dataset.

Approach	SBP(mmHg)		DBP(mmHg)	
	MAE	Std	MAE	Std
Baek et al. [2]	17.71	–	11.27	–
Rong et al. [19]	16.75	20.42	11.21	13.80
Zhou et al. [27]	16.31	19.79	11.17	13.97
AlexNet*	18.17	21.05	11.50	14.02
ResNet-50*	17.07	21.21	11.83	14.21
SVR*	17.30	21.13	10.93	13.50
S2-Net*	16.27	20.38	11.83	14.02
FS2-Net*	16.01	12.89	10.97	8.27
Ours (Baseline)	15.59	10.63	10.77	7.41
Ours (w/ $M(\cdot)$)	10.15	8.75	8.84	6.52
Ours (w/ InfoGAN)	**9.13**	**8.18**	**8.76**	**6.13**

* The results are referred to [24].

Finally, we conduct the experiment which includes model selection and synthetic data generation procedures. The MAE reduces significantly to 9.13 mmHg than the results of other end-to-end rPPG-based models.

Similarly, the standard deviation of the MAE diminishes to less than one-half with the proposed method. Take FS2-Net [24] for example again, the proposed method improves

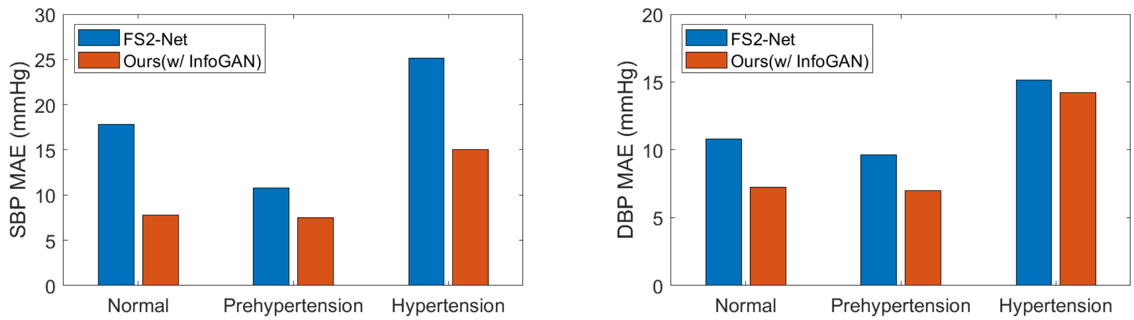

(a) SBP MAE (b) DBP MAE

Figure 7. The error comparison of three groups, including normal, prehypertension, and hypertension. between the proposed method and FS2-Net [24]. (a) is the error of SBP and (b) is for DBP.

the results for the participants with normal or hypertension blood pressure. With the diagram shown in Figure 7, it is easily observed that the FS2-Net can only handle the blood pressure values which lie in the middle range like the prehypertension group. This observation is consistent with the issue of bounded output which is solved significantly with our approach.

4. Conclusion

A CNN-based contactless blood pressure estimation is proposed in this study. Our backbone model achieves comparable results on the PPG datasets to the state-of-the-art PPG-based methods. Besides, model selection mechanism and synthetic data generation are addressed to deal with the issues of bounded output and the lack of data, especially in the rPPG case. With the experimental results, there is a significant improvement both in MAE and the standard deviation of the error. That is, the proposed method elevates the performance of the hypertension group efficiently.

In the future, this contactless measurement is expected to extend to the nighttime blood pressure monitoring for ease of interference. For eliminating the dependency of visible light, the rPPG construction under infrared light conditions should be considered so that the knowledge between the rPPG signals and the blood pressure so far can be adopted. Besides, the preprocessing to obtain better rPPG is indispensable due to the interference from the head movement.

5. Acknowledgement

This work was supported by the Ministry of Science Technology under Grant no. MOST 110-2221-E-A049-125. The rPPG Dataset used in this work is cooperated with Chang Gung Medical Foundation, Taiwan, and approved by institutional review board under no. 201900668B0C502.

References

[1] Ahmadreza Argha, Branko G. Celler, and Nigel H. Lovell. A novel automated blood pressure estimation algorithm using sequences of korotkoff sounds. *IEEE Journal of Biomedical and Health Informatics*, 25(4):1257–1264, 2021. 1

[2] Sanghyun Baek, Jiyong Jang, and Sungroh Yoon. End-to-end blood pressure prediction via fully convolutional networks. *IEEE Access*, 7:185458–185468, 2019. 7

[3] Daniel Barvik, Martin Cerny, Marek Penhaker, and Norbert Noury. Noninvasive continuous blood pressure estimation from pulse transit time: A review of the calibration models. *IEEE Reviews in Biomedical Engineering*, 15:138–151, 2022. 1

[4] Ayan Chakraborty, Dharitri Goswami, Jayanta Mukhopadhyay, and Saswat Chakrabarti. Measurement of arterial blood pressure through single-site acquisition of photoplethysmograph signal. *IEEE Transactions on Instrumentation and Measurement*, 70:1–10, 2021. 1

[5] Xi Chen, Yan Duan, Rein Houthooft, John Schulman, Ilya Sutskever, and Pieter Abbeel. Infogan: Interpretable representation learning by information maximizing generative adversarial nets. *Advances in neural information processing systems*, 29, 2016. 2, 3, 4

[6] Gerard de Haan and Vincent Jeanne. Robust Pulse Rate From Chrominance-Based rPPG. *IEEE Transactions on Biomedical Engineering*, 60(10):2878–2886, 2013. 3

[7] Serj Haddad, Assim Boukhayma, and Antonino Caizzone. Continuous ppg-based blood pressure monitoring using multi-linear regression. *IEEE Journal of Biomedical and Health Informatics*, pages 1–1, 2021. 1

[8] Chuanqi Han, Mengyin Gu, Fang Yu, Ruoran Huang, Xi Huang, and Li Cui. Calibration-free blood pressure assessment using an integrated deep learning method. In *2020 IEEE International Conference on Bioinformatics and Biomedicine (BIBM)*, pages 1001–1005, 2020. 2

[9] Kaiming He, Xiangyu Zhang, Shaoqing Ren, and Jian Sun. Deep residual learning for image recognition, 2015. 2

[10] Da Un Jeong and Ki Moo Lim. Combined deep cnn-lstm network-based multitasking learning architecture for nonin-

vasive continuous blood pressure estimation using difference in ecg-ppg features. *Scientific Reports*, 11(1):1–8, 2021. 1

[11] Alistair EW Johnson, Tom J Pollard, Lu Shen, Li-wei H Lehman, Mengling Feng, Mohammad Ghassemi, Benjamin Moody, Peter Szolovits, Leo Anthony Celi, and Roger G Mark. Mimic-iii, a freely accessible critical care database. *Scientific data*, 3(1):1–9, 2016. 5, 6

[12] Mohamad Kachuee, Mohammad Mahdi Kiani, Hoda Mohammadzade, and Mahdi Shabany. Cuff-less high-accuracy calibration-free blood pressure estimation using pulse transit time. In *2015 IEEE International Symposium on Circuits and Systems (ISCAS)*, pages 1006–1009, 2015. 5, 6, 7

[13] Cederick Landry, Eric T. Hedge, Richard L. Hughson, Sean D. Peterson, and Arash Arami. Accurate blood pressure estimation during activities of daily living: A wearable cuffless solution. *IEEE Journal of Biomedical and Health Informatics*, 25(7):2510–2520, 2021. 1

[14] Jing Liu, Shirong Qiu, Ningqi Luo, Sze-Kei Lau, Hui Yu, Timothy Kwok, Yuan-Ting Zhang, and Ni Zhao. Pca-based multi-wavelength photoplethysmography algorithm for cuffless blood pressure measurement on elderly subjects. *IEEE Journal of Biomedical and Health Informatics*, 25(3):663–673, 2021. 1

[15] Jing Liu, Charles G. Sodini, Yanghui Ou, Bryan Yan, Yuan-Ting Zhang, and Ni Zhao. Feasibility of fingertip oscillometric blood pressure measurement: Model-based analysis and experimental validation. *IEEE Journal of Biomedical and Health Informatics*, 24(2):533–542, 2020. 1

[16] Jing Liu, Bryan P. Yan, Yuan-Ting Zhang, Xiao-Rong Ding, Peng Su, and Ni Zhao. Multi-wavelength photoplethysmography enabling continuous blood pressure measurement with compact wearable electronics. *IEEE Transactions on Biomedical Engineering*, 66(6):1514–1525, 2019. 1

[17] Adam Paszke, Sam Gross, Francisco Massa, Adam Lerer, James Bradbury, Gregory Chanan, Trevor Killeen, Zeming Lin, Natalia Gimelshein, Luca Antiga, et al. Pytorch: An imperative style, high-performance deep learning library. *Advances in neural information processing systems*, 32:8026–8037, 2019. 5

[18] Alexandru-Gabriel Pielmuş, Maik Pflugradt, Timo Tigges, Michael Klum, Aarne Feldheiser, Oliver Hunsicker, and Reinhold Orglmeister. Novel computation of pulse transit time from multi-channel ppg signals by wavelet transform: Towards continuous, non-invasive blood pressure estimation. *Current Directions in Biomedical Engineering*, 2(1):209–213, 2016. 1

[19] Meng Rong and Kaiyang Li. A blood pressure prediction method based on imaging photoplethysmography in combination with machine learning. *Biomedical Signal Processing and Control*, 64:102328, 2021. 2, 7

[20] Fabian Schrumpf, Patrick Frenzel, Christoph Aust, Georg Osterhoff, and Mirco Fuchs. Assessment of non-invasive blood pressure prediction from ppg and rppg signals using deep learning. *Sensors*, 21(18):6022, 2021. 2, 5, 6

[21] Gašper Slapničar, Nejc Mlakar, and Mitja Luštrek. Blood pressure estimation from photoplethysmogram using a spectro-temporal deep neural network. *Sensors*, 19(15):3420, 2019. 1, 6

[22] Peng Su, Xiao-Rong Ding, Yuan-Ting Zhang, Jing Liu, Fen Miao, and Ni Zhao. Long-term blood pressure prediction with deep recurrent neural networks. In *2018 IEEE EMBS International Conference on Biomedical Health Informatics (BHI)*, pages 323–328, 2018. 1

[23] Ryo Takahashi, Keiko Ogawa-Ochiai, and Norimichi Tsumura. Non-contact method of blood pressure estimation using only facial video. *Artificial Life and Robotics*, 25(3):343–350, 2020. 1

[24] Bing-Ruei Tsai and Bing-Fei Wu. A calibration-free and facial-image-based blood pressure measurement system. *[Unpublished master's thesis], National Yang Ming Chiao Tung University*, 2021. 2, 7, 8

[25] Seungman Yang, Jangjay Sohn, Saram Lee, Joonnyong Lee, and Hee Chan Kim. Estimation and validation of arterial blood pressure using photoplethysmogram morphology features in conjunction with pulse arrival time in large open databases. *IEEE Journal of Biomedical and Health Informatics*, 25(4):1018–1030, 2021. 1

[26] Pandeng Zhang, Chang Liu, Haibo Chen, and Jia Liu. Reconstruction of continuous brachial arterial pressure from continuous finger arterial pressure using a two-level optimization strategy. *IEEE Transactions on Biomedical Engineering*, 67(11):3173–3184, 2020. 1

[27] Yimin Zhou, Haiyang Ni, Qi Zhang, and Qingtian Wu. The noninvasive blood pressure measurement based on facial images processing. *IEEE Sensors Journal*, 19(22):10624–10634, 2019. 2, 7